GLOBAL JOURNAL OF PURE AND APPLIED SCIENCES VOL. 13, NO. 2, 2007: 227 - 236
COPYRIGHT (C) BACHUDO SCIENCES CO. LTD. PRINTED IN NIGERIA. 1SSN 1118-0579

VARIABLE TIME AND SPACE STEPS (VTSS) SOLUTION OF A TWO-PHASE MOVING BOUNDARY PROBLEM IN CYLINDRICAL COORDINATES

A. OUEDRAOGO AND J. C. MULLIGAN

(Received 18 November 2005 ; Revision Accepted 13 September 2006)

ABSTRACT

Equations of a two-phase moving boundary problem in cylindrical coordinates are obtained from the formulation of a transient shrinking core model of whole tree combustion in a one-dimensional steady state fixed-bed reactor. A hybrid Variable Time and Space Steps (VTSS) method is developed to solve the non linear equations and the results are compared with those of the literature and whole tree quasi-steady combustion model. The transient and the quasi-steady models predict respectively 45 and 41.42 min burnout times, which are quite similar to the 40 min obtained by the Research Triangle Institute (RTI) when combusting whole tree of 10 cm radii at 33.3% moisture content. The elapsed time shown by the actual model is believe to be due to the blowing of moisture at the combustion front inducing chilling and retarding effects on the combustion rate. In the meantime, the same reference selected deep bed combustion of 3.65 m depth, up from an extrapolated shallow bed of 1.30 m, while the transient model predicts a computed coal-like bed of 2.60 m. Hence, to accommodate for bigger whole tree radii and higher moisture content, a tradeoff deep combustion bed depth of 4.50 m has been chosen. To meet the increasing environmental requirements, whole tree boilers may become attractive either alone or co-firing with coal because biomass is very low in sulfur content and nearly a net zero CO_2 generator over the long term.

KEYWORDS: Combustion, Fixed-bed, Moving boundary, Shrinking core, Whole tree

NOMENCLATURE

A_b	bed cross section (m^2)
A_m	pre-exponential factor (s^{-1})
C_{pj}	specific heat of component j kJ/(kg. K)
E	activation energy (J/mole)
h	heat transfer coefficient kJ/(m^2 .s .K)
h_p	heat of pyrolysis (kJ/kg)
k_{gc}	permeability of the gases in the core (m^2)
k_{gs}	permeability of gases in the shell (m^2)
Lr	dry fuel rate (kg/s)
mc	moisture content (%)
P	pressure (Pa)
r	radius (m)
r_o	initial radius (m)
R	gas constant J/(mole K)
t	time (s)
T	temperature (^oC)
T^*	Pyrolysis (moving boundary) or interface shell-core Temperature
V_g	gas convective velocity (m/s)
V_s	rate of shell recession (m/s)
V_{sg}	superficial gas velocity (m/s)
z	bed coordinate (m)

GREEK LETTERS

ε	mass fraction
Φ_s	bed solid fraction
ρ	density (kg/m^3)
ϕ	wood porosity
μ	viscosity

Ouedraogo, Unit of Formation and Res. in Exacts and Applied Sci. Univ. of Ouagadougou, Bp 7021 Ouagadougou, Burkina Faso.
C. Mulligan, Department of Mechanical and Aerospace Engineering, North Carolina State University, Raleigh, NC 27695-7910

SUBSCRIPTS

a	atmospheric
c	core
d	dried wood
g	gas
m	moisture
s	shell (external radius)
v	volatile
w	virgin wood

INTRODUCTION

This paper reports the second part of ongoing investigations on an actual under-fired whole tree fixed-bed, with fuel rate totaling 56.50 ton/h (dry basis). The fuel bed with a pressure of 1 atmosphere and length, width and depth respectively equal to 9.144, 4.572 and 4.572 m, rests on a water-cooled fixed grate designed to fire a 100 MW whole tree power plant. The previous work, Ouédraogo et al. (2000), based on the formulation of a shrinking core model assumes the following: one-dimensional steady state fuel bed with quasi-steady conditions prevailing in each fuel element, which shrinks and migrates through the bed with a velocity V_f in rows of N fuel elements at a frequency of V* rows/esc, countercurrent to the preheated gas fed from the bottom. Now, the actual model differs from the previous due to the assumption of transient conditions in each fuel element. The logs, which are loaded uniformly into the bed utilizing large crane, are then believed to go through overlapping phases of heating, pyrolysis and combustion. Consequently, three distinct layers are formed: the burning char layer, the dried pyrolyzing layer and the core layer, separated by two interfaces or moving boundaries together with the external receding combustion front. To simplify the model, however, it can be assumed that the pyrolysis layer is so thin that it may be neglected, Figure 1.

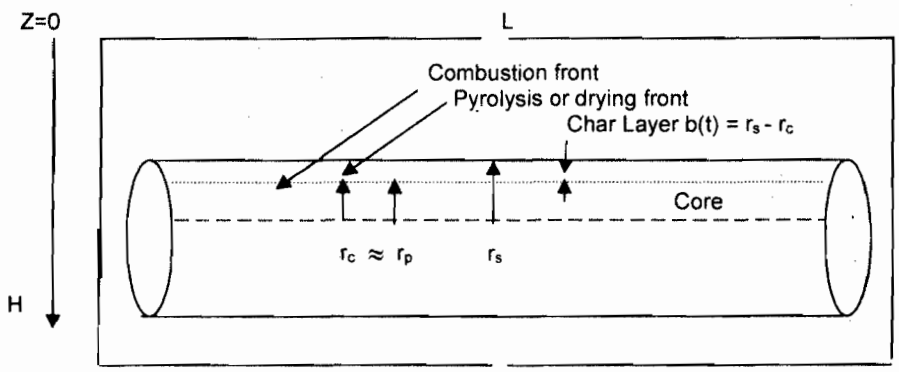

Figure 1: Whole tree fuel combustion model

The objective of the study is to upgrade the results of the quasi-steady model thus, providing better whole tree combustion data of fuel burnout time, combustion depth and fuel temperature as function of fuel properties and flow characteristics, for a better estimate of boiler wood heat release rate and efficiency.

THE BED UPPER REGION SUBMODEL : HEATING AND PYROLYSIS

The upper region goes from the bed inlet (z=0) down to the plan $z=z_p$ where the first char layer is formed. The whole tree element assumed to be at uniform ambient temperature is loaded into a continuously operating countercurrent fixed-bed. The fuel element is also assumed to be made of fixed carbon (shell), active matter that pyrolyzes to volatile gases and moisture, which phase-changed to water vapor. The model is developed with the understanding that there is no viscous dissipation, wood thermal conductivity is taken constant and only radial movement of moisture and volatile gases occurs. Each phase represents a continuum governed by conservation laws and hence, (Whitaker, 1977), a single governing equation may be achieved which is valid throughout all phases by phase averaging; consequently, the phase averaged solid energy equation is governed by

$$\phi\rho_w(\varepsilon_s C_{ps} + \varepsilon_v C_{pv} + \varepsilon_m C_{pm})\frac{\partial T}{\partial t} + \rho_w \varepsilon_m C_{pm} V_g \frac{\partial T}{\partial r} = \frac{1}{r}\frac{\partial}{\partial r}(rK_w \frac{\partial T}{\partial r}) - Q \quad (1)$$

$$Q = \varepsilon_m(\rho_w - \rho_d)(1-\phi)hpc_m A_m \exp(-E_m / RT)$$; (Aerta D. J. et al. 1990).

The steady state gas energy equation is approximated as

$$\rho_g C_{pg} V_{sg} \frac{\partial T_g}{\partial z} = \frac{d}{dz}\left(K_g \frac{dT_g}{dz}\right) hA_{av}(T_g - T(r_s,t)) + Q \quad (2)$$

The conservation of mass equation is modeled as follows, (Dinwoodie, 1997).

$$\rho_w = S_g(1+mc)\rho_m$$

While, the momentum equation is given by the Darcy's law, that is

$$V_g = -\frac{k_{gc}}{\mu_g}\nabla P_g(r)$$

where the pressure is taken to be saturated vapor pressure. The above set of equations is subjected to the following initial and boundary conditions

$$T(r, t=0) = T_i \qquad 0 \le r \le r_0$$

$$\left.\frac{\partial T}{\partial r}\right|_{r=0} = 0 \qquad t \phi 0$$

$$K_w \left.\frac{\partial T}{\partial r}\right|_{r_O} = h(T_g - T(r_o, t)) \qquad t \phi 0$$

At the end of the heating and pyrolysis process ($z=z_p$ and $t=t_p$), a char layer of thickness b ($t = t_p$) is formed surrounding a core or virgin wood of radius r_c, figure 2a.

Char Layer b(t) = r_s - r_c

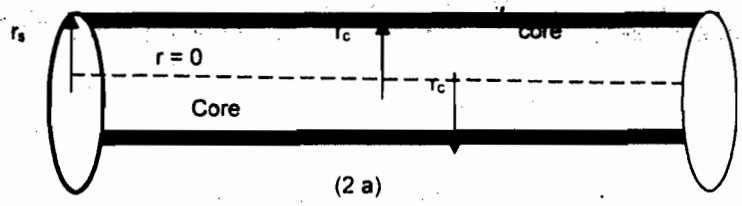

(2 a)

SOLID PHASE MODELING: SHELL COMBUSTION

At this point of the bed ($z = z_p$), the combustion conditions prevail i.e.: fuel, adequate oxygen concentration and inignition temperature exist. Hence, the combustion of the shell layer begins and takes place at constant density. The volatile gases and the water vapor leaving the drying and pyrolyzing core, convect through the porous shell into the bed environment. Heat is generated only by glowing combustion at the shell-gas interface. Hence, the phase averaged solid shell layer energy equation is written as

$$\phi\rho_s C_{ps}\frac{\partial T_s}{\partial t} + \rho_w V_g(\varepsilon_v C_{pv} + \varepsilon_m C_{pm})\frac{\partial T_s}{\partial r} = \frac{1}{r}\frac{\partial}{\partial r}(rK_s\frac{\partial T_s}{\partial r}) \qquad (3)$$

The convective boundary equation at the combustion front ($r = r_s$) is modeled as

$$\rho_w(V_s\varepsilon_s h_s + \alpha V_g \varepsilon_v h_v) + h(T_g - T_s(r=r_s,t)) = K_s\left.\frac{\partial T_s}{\partial r}\right|_{r=r_s} \qquad t \phi t_p$$

where h and V_g have been correlated previously (Ouédraogo et al., 1998). Here, the gases convect at a much higher velocity. Since there is no moisture inside the shell layer, the vapor pressure $P(r)$ is not sutured and is modeled as shown

$$P(r) = P_g + (P_a - P_g)\frac{\ln(r/r_c)}{\ln(r_s/r_c)} \qquad (4)$$

where P_g and P_a, the inner and outer limits of the actual pressure, are respectively the saturated vapor pressure and the atmospheric pressure. Finally, at the core-shell interface, the temperature is prescribed and is equal to the interface or moving boundary temperature T^*

$$T_s(r=r_c,t) = T^* \qquad t \phi t_p$$

THE DRYING CORE

A fraction of the heat generated by the combustion and the moisture evaporated by the pyrolysis, propagate inward; together, they not only further dry and pyrolyze the core which is made of virgin wood, but also increases the core temperature and pressure (effect of cooking). The set of conservative equations in the core is similar to the heating equations (1) and hence, will not

be repeated However, the initial temperatures are given by the core temperature profiles at the end of the heating process. As for the boundary conditions, we have zero heat flux at the logs midplane and prescribed temperature at the core-shell interface, that is:

$$T_c(r = r_c, t) = T_s(r = r_c, t) = T^* \qquad t \phi t_p$$

EQUATIONS OF THE MOVING BOUNDARY

This equation is obtained by performing an energy balance at the core-shell interface

$$K_s \frac{\partial T_s}{\partial r} - K_w \frac{\partial T_c}{\partial r} = -\rho_w r_c \varepsilon_s h_p \qquad (5)$$

Where $-r_c = V_c$ is the core recession velocity and h_p the heat of pyrolysis, neglecting the heat of evaporation of moisture and its effect on the propagation of the pyrolysis wave. Relation (5) is a moving boundary equation since the shell-core interface changes its position continuously due to pyrolysis with the subsequent phase-change of the active matters (shell) and moisture (core) respectively to volatile gases and water vapor. The core and shell temperatures are different throughout, hence, the problem is a two phase-change or a two-phase moving boundary problem, sometimes referred to simply as "Stefan problem", figure 2b and 2c.

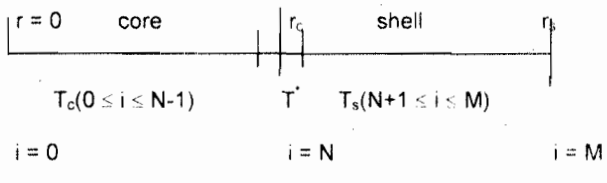

(2 b)

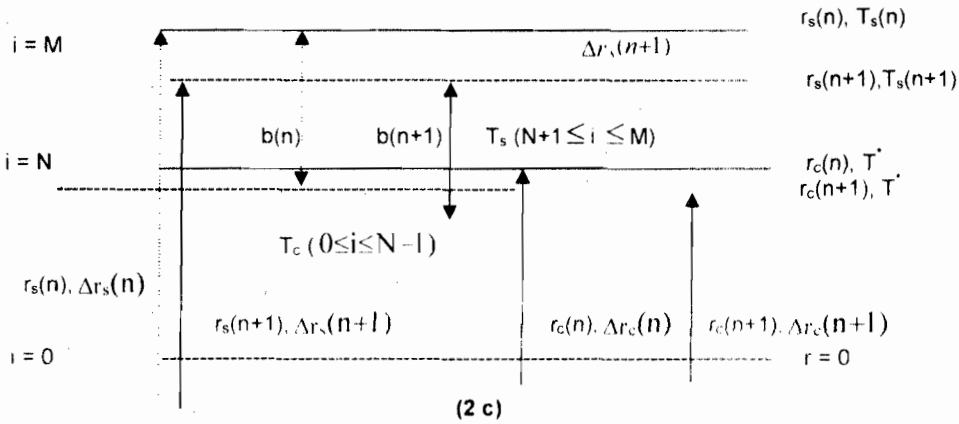

(2 c)

Figure 2 : Computational domain

SIMPLIFIED GAS PHASE COMBUSTION

The products of the incomplete combustion at the char-gas interface, CO for the most part, and the fraction of the volatiles that may have escaped earlier in the combustion now go into complete combustion in the gas phase. The preheated air with maximum prescribed concentration at the bottom of the bed moves in countercurrent to the flow of solid fuel. Since the steady state conditions prevailing in the bed have been modeled previously (Ouédraogo et al., 2000), these equations will not be repeated here.

VARIABLE TIME AND SPACE STEPS (VTSS) SOLUTION OF THE MOVING BOUNDARY PROBLEM

The set of equations to be solved are nonlinear due to the nonlinearity of the governing equations and boundary conditions and their solutions can be obtained by numerical finite difference methods. The flow problem can be decoupled from the temperature problem so that the radial velocity V_g becomes an input to the energy equation. Using the Combined Crank-Nicolson (CCN) method, the discretization of these equations is straightforward and sample calculations are given in the appendix. Assuming that the values of the coefficients of the temperatures are available and choosing appropriate constant time step and initial temperatures, the determination of the fuel unknown temperatures and shell thickness at the end of the heating and pyrolysis process (equation 1) are done by using the CCN scheme. Now, this scheme alone is not sufficient for the determination of the core and shell temperatures; figure 2 shows clearly the two subdomains. While the discretization of their respective equations is similar, the time step, however, is not constant anymore and must be obtained by discretizing equation (5) as follows:

$$t_n - t_{n+1} = \Delta t_n = \frac{\rho_w \varepsilon_w h_p \Delta r^2}{K_w [T^* - T_{c,N-1}^{n+1}] - K_s [T_{s,N+1}^{n+1} - T^*]} \quad (6)$$

The bed grid size is inferred from equation (6) as

$$\Delta z_k = \Delta t_n \left[\frac{L r}{(1-mc)(\rho_w A_b \Phi_s)} \left(\frac{r}{r_o} \right)^2 \right] \quad (7)$$

As can be seen, the bed grid size is dependant on the time step of the moving boundary and therefore, the VTSS is a hybrid method. To handle the moving boundary problem, various techniques and numerical schemes have been reported in the literature by many investigators, a classification of these methods can be found in the book by Ozisik (1994). Here however, a modified version of the Variable grid methods called Variable Time and Space Steps (VTSS) method is presented for solving the "Stefan problem". Under the previous methods, such as those by Murry and Landis (1959), Douglas and Gallie (1995) and Gupta and Kumar (1981), usually a plane geometry domain "x-t" is subdivided into equal interval in one direction only, the other grid size being determined so that the moving boundary always remains at a grid point. In the actual method, each subdomain of figure 2 (core and shell) is divided at the beginning of the combustion process into equal intervals in space only by fixing the number of grid points, N and M respectively. Therefore, their mesh sizes change as the interface and the external boundary move, figure 2 c. The following relations summarize this approach during one time step:

Core r_c ($0 \leq n \leq N-1$), shell r_s ($N+1 \leq n \leq M$)

At t_n

Core: $r_c(n) = N\Delta r_c(n)$ and $\Delta r_c(n) = r_c(n) / N$

Shell: $b(n) = M\,\Delta r_s(n)$ and $\Delta r_s(n) = b(n) / M$

At t_{n+1}

Core: $r_c(n+1) = r_c(n) - \Delta r_c(n) = N\Delta r_c(n+1)$ and $\Delta r_c(n+1) = r_c(n+1) / N$

Shell: $b(n+1) = r_s(n+1) - r_c(n+1) = M\,\Delta r_s(n+1)$ and $\Delta r_s(n+1) = b(n+1)/M$

Where $r_s(n+1)$ is inferred from the iteration of the shell recession velocity V_s.

$$V_s(n) = \frac{r_s(n+1) - r_s(n)}{\Delta t_n}$$

Next, the time step Δt_n is obtained such that both the moving boundary and the external receding combustion front remain each at a grid point. The determination of the temperature profiles at (t_{n+1}) is done given the previous temperature profiles (t_n), that is

$$[T_c^{n+1}(0 \leq i \leq N-1), \Delta r_c(n+1), \Delta t(n+1)] \rightarrow [T_c^n(0 \leq i \leq N-1), \Delta r_c(n), \Delta t(n)]$$

$$[T_s^{n+1}(N+1 \leq i \leq M), \Delta r_s(n+1), \Delta t(n+1)] \rightarrow [T_s^n(N+1 \leq i \leq M), \Delta r_s(n), \Delta t(n)]$$

RESULTS AND DISCUSSIONS

At the end of the heating and pyrolysis process, solved solely with the CCN discretized equations, a dried pyrolyzing layer of thickness equal to 6 mm is obtained, figure 1. Now, for the combustion of this layer, which is the second process, figure 2, the VTSS method, is used, that is, the CCN and the moving boundary discretized equations together with the constant thermal properties. Table I

TABLE I : Constant thermal properties

Properties	Values	Units	References
A_m	1.08×10^7	sec^{-1}	Chan, R et al.
C_{ps}	0.670	kJ/(kg-K)	Hsiang-Cheng et al.
C_{pv}	1.10	kJ/(kg-K)	Hsiang-Cheng et al
E_m	5.60×10^4	J/mol	Chan, R et al.
hpc_m	2250	kJ/kg	
H_s	31, 100	kJ/kg	Hsiang-Cheng et al
K_s	0.41×10^{-4}	kW/(m-K)	Hsiang-Cheng et al
K_w	1.254×10^{-4}	kW/(m-K)	Hsiang-Cheng et al.
K_{gc}	56.0×10^{-19} / 5.00×10^{-19}*	m^2	Fredlund B.
K_{gs}	15.0×10^{-17} / 12.0×10^{-16}*	m^2	Fredlund B.
ρ_S	95	kg/m^3	Ragland et al.
ϕ	0.45	-	Aerta et al.
μ_g	38.1×10^{-6} / 40.0×10^{-6}*	$kgm^{-1} sec^{-1}$	Fredlund B.

* best fit

During the combustion of the solid fuel elements, their radii shrink from r_o at the boiler inlet to r_f (95% of r_o) when they fall through the fixed grate grill holes into the ash pit. Of particular importance for wood boiler furnaces design are the burnout time (t_b) and the combustion zone depth (z_p), which are respectively, the logs actual residence time and their vertical traveled distance inside the bed, which corresponds to the shallow bed depth.

As expected and for the two models, these characteristics are shown to increase first, moderately at low moisture content and small fuel radii, then quite faster when these properties become large, fuel radii being more sensitive to the variations than their moisture contents do. For small whole tree radii, 7.5 cm, the burnout time and bed depth are approximately constant, independent of model type. Now, direct comparison indicates that retarding effects due to moisture content on the burning rate are more pronounced with the transient model. With whole tree of 15.24 cm radii at 25 and 40 % moisture contents, Table II data indicate burning rates ranging from 2.08 to 1.86 and from 2.01 to 1.65 mm/min respectively for the quasi-steady and the transient models, showing a retarding coefficient of 1.6.

TABLE II . **The burnout times (s) of the two models**

r_o (m)	mc (%) 25		30		33.3		40	
	Steady State	Transient	Steady State	Transient	Steady State	Transient	Steady State	Transient
0.075	23.88	23.69	24.88	25.46	25.52	27.16	26.80	28.80
0.1016	38.86	39.30	40.42	42.42	41.42	45.09	43.50	48.12
0.1524	73.24	75.52	76.10	80.81	78.00	85.93	81.92	92.38
0.2032	115.26	118.91	119.76	127.96	122.74	135.99	128.90	146.35
0.2540	163.86	169.25	170.20	182.04	174.45	193.99	183.20	209.29

Unfortunately, there are few models of large wood combustion models in the literature; most models deal either with kinetics of wood pieces or with fixed-bed gasifier. Ragland et al. (1998) reported a model results of 0.075 m radius chunk wood combustion; they were predicted to burnout in 32 min at rate of 1.8 mm/min, function of fuel radius but independent of initial moisture content. The same paper indicated, however, a calculated char layer thickness respectively equal to 6 mm and 10 mm for green and air-dried wood after 5 min in furnace, implying moisture dependence. As a matter of fact, Mardani et al. (1993), found moisture content to increase the ignition time of wood due to the energy used to evaporate additional water. In addition, another retarding factor is the chilling effect of moisture due the blowing at the combustion front, Ouédraogo et al. (1998), which abates the combustion temperature, hence slowing down the burning rate. This phenomenon, which increases with moisture content and not taken in account by the quasi-steady model, may explain the burnout time difference of the two models. Utilizing the best combustion models available to extrapolate for larger wood and higher moisture contents, and data from the actual water-cooled fixed bed, the Research Triangle Institute (TRI, 1991) reached a compromise burnout time of 40 min, for whole tree of 10 cm radius and 33.3 % moisture content, which is quite similar to the results of these models (41.42 and 45 min, Table II). For the fuel bed, the RTI found

an extrapolated shallow bed of about 1.30 m and compromise deep bed combustion of 3.65 m depth based on whole tree tests results conducted at Bay Front and St John's (cited by RTI). Those are quite similar to the fuel bed ranges predicted by the two models, Table III.

TABLE III : **The bed depths (m) of the two models**

r_o (m)	mc (%)							
	25		30		33.3		40	
	Steady State	Transient	Steady State	Transient	Steady State	Transient	Steady State	Transient
0.075	1.88	1.41	1.96	1.51	2.01	1.61	2.10	1.69
0.1016	3.07	2.30	3.19	2.46	3.26	2.60	3.41	2.74
0.1524	5.78	4.34	6.00	4.60	6.14	4.84	6.42	5.08
0.2032	9.10	6.80	9.44	7.20	9.66	7.56	10.10	7.94
0.2540	12.93	9.65	13.41	10.20	13.72	10.72	14.35	11.23

As a matter of fact, the 3.26 m of the quasi-steady model is that of deep bed combustion, that is, the logs are let to shrink up to 99% of initial radii, while the reported 2.60 m of the transient model represents only 95 % of initial shrinking radii, the fuel mesh size becoming too thin ($\Delta r = 10^{-10}$cm) for the computation to proceed. Hence, a tradeoff value of 4.50 m deep bed combustion has been selected based on data of the transient model and the compromised model of the RTI.

Now, a heat of pyrolysis of 84 J/g was computed as a best fit for the variable time step; Wai-Chun R Chan et al. (1985) reported that, the heats of reaction for wood thermolysis are not well known and have been observed to range from – 418 to + 418 $kJkg^{-1}$.

With the advent of environmental pollution control, whole tree boilers may become attractive either alone or preferably in co-firing with coal. The energy density and low heating value of biomass fuel require, however, that relative to coal, the combustion area be oversized for deep bed combustion. Because biomass is very low in sulfur content and nearly a net zero CO_2 generator over the long term, it can displace the energy supplied by coal while reducing emissions. According to Edward E. Gray (1991), if a unit was required to cut its SO_2 emissions by 15 % or voluntarily agreed to reduce CO_2 emissions the same amount, the unit could co-fire roughly 15 % biomass (on a heat input basis) and 85% coal to meet the restrictions.

CONCLUSION

At moderate moisture content and relatively small radii, the two models show similar burnout time and combustion bed depth. For these sizes, the whole tree-shrinking rate is quite constant as stated by Ragland et al. (1998). But the influence of these properties over the whole tree combustion characteristics becomes sensible especially with large wood radii and higher moisture content. As a matter of fact, the migration of the inner moisture up to the external surface is function of the localization of the combustion front and its temperature; the energy require to evaporate the moisture increases with moisture (Mardini et al.) as does the blowing, with chilling and retarding effects on the combustion front. Hence, a retarding coefficient approximately equal to 1.6 has been observed between the two-burnout times. Taking in account the comparatively low heating value of wood, a bed deep combustion of 3.65 m depth has been selected by the RTI, up from computed shallow fuel bed of 1.30 m. In the meantime, up from a coal-like fuel bed of 2.60 m depth, oversized deep bed combustion of 4.50 m depth has been chosen using the transient model in order to guaranty adequate combustion of bigger whole tree radii and higher moisture content.

REFERENCES

Aerta D. J. and Ragland K.W., 1990. Pressurized downdraft combustion of woodchips, Twenty-third Symposium (International) on Combustion. The Combustion Institute: 1025-1032.

Chan R.W., Kelbon M. and Krierger B. B., 1985. Modeling and experimental verification of physical and chemical processes during pyrolysis of a large biomass particle, FUEL 64:1505-1513

Dinwoodie J., 1997.Nature's cellular, polymeric fibre- composite. The Institute of Metals:3-37

Douglas J. Jr and Gallie T M Jr., 1995. On the numerical integration of a parabolic differential equation subject to a moving boundary condition, Duke Math. Jl 22: 557-570.

Fredlund B., 1998. A model for heat and mass transfer in timber structures during fire. A theoretical, numerical and experimental study, Ph.D. Thesis, Institute of Science and Technology, Lund University Sweden

Gupta R. S. and Kumar D., 1981.Variable time step methods for one-dimensional Stefan problem with mixed boundary condition, J. Heat and Mass Transfer 24:251-259.

Hsiang-Cheng K. and Kalelkar S. A., 1985. On the heat of reaction in solid-convective heat transfer environments, In: Fundamentals of thermochemical biomass conversion. R. P.Overend T. A. Milne and L. K. Mudge (Editors). Elsevier Applied Sciences Publishers, pp. 539-555

Mardini J. A., Lavine A. S. and Dhir V. K., 1993. On the effects of the governing parameters on the time to ignition and weight loss of a simulated fuel element during a fire, ASME Paper 93-WA/HT-45: 1-9

Murry W. D. and Landis F., 1959. Numerical and machine solutions of transient heat conduction problems involving melting or freezing, Transactions of the ASME 81:106-112

Ouédraogo A., Mulligan J. C and Cleland J. G., 2000. A quasi-steady state shrinking core model of whole tree combustion in a countercurrent fixed-bed, J. Recher. Sci. Univ. Bénin. 4 (2): 199-208

Ouédraogo A., Mulligan J. C. and Cleland J. G., 1998. A quasi-steady shrinking core analysis of wood combustion, Combustion and Flame.114:1-12

Ozisik M. N., 1994. Finite Difference Methods in Heat Transfer, CRC Press, inc. Vol 1

Ragland K. W., Boeger J. C. and Baker A. J., 1972. A model of chunk wood combustion. Forest Products Journal. 38 (2): 27-32

Research Triangle Institute, 1991. Whole tree energy: Engineering and economic evaluation, Draft Final Report EPRI Project RP2612-15

Whitaker S., 1977. Simultaneous heat, mass and momentum transfer in porous media: A theory of drying, Adv. Heat Transfer 9:119-203

APPENDIXES: DISCRETISATION OF THE MODEL EQUATIONS

Let's write the general form of the diffusion equations (1 and 3) as follows:

$$\varphi\rho C_p\frac{\partial T}{\partial t}+\lambda(T)\frac{\partial T}{\partial r}=\frac{1}{r}\frac{\partial}{\partial r}(rK\frac{\partial T}{\partial r})+Q(T) \qquad (8)$$

CCN DISCRETIZED EQUATIONS

Internals nodes

In figure 2 b, the internal nodes are respectively $1\pi i\leq N-1$ and $N+1\leq i\leq M-1$ for the core and shell regions; i=0 needs a special treatment because of the singularity problem and will be addressed latter. Applying the simple explicit forward differencing for the time derivative, the upwing and the central differencing schemes to discretize respectively the convective terms and the second order derivatives, the following finite difference approximation of the general diffusion equation is obtained (9a).

$$-[\frac{\Delta t\Theta\lambda(T_i^n)}{(\phi\rho C_p)_i\nabla r}+\frac{\Delta t\Theta(rK)_{i-1/2}}{(r\phi\rho C_p)_i\Delta r^2}]T_{i-1}^{n+1}+[1+\frac{\Delta t\Theta(rK)_{i+1/2}}{(r\phi\rho C_p)_i\Delta r^2}+\frac{\Delta t\Theta(rK)_{i-1/2}}{(r\phi\rho C_p)_i\Delta^2}+\frac{\Delta t\Theta\lambda(T_i^n)}{(\phi\rho C_p)_i\Delta r}]T_i^{n+1}$$

$$-\frac{\Delta t\Theta(rK)_{i+1/2}}{(r\phi\rho C_p)_i\Delta r^2}T_{i+1}^{n+1}=[\frac{\Delta t(1-\Theta)\lambda(T_i^n)}{(\phi\rho C_p)_i\Delta r}+\frac{\Delta t(1-\Theta)(rK)_{i-1/2}}{(r\phi\rho C_p)_i\Delta r^2}]T_{i-1}^n+[1-\frac{\Delta t(1-\Theta)(rK)_{i+1/2}}{(r\phi\rho C_p)_i\Delta r^2}$$

$$-\frac{\Delta t(1-\Theta)(rK)_{i-1/2}}{(r\phi\rho C_p)_i\Delta r^2}-\frac{\Delta t(1-\Theta)\lambda(T_i^n)}{(\phi\rho C_p)_i\Delta r}]T_i^n+\frac{\Delta t(1-\Theta)(rK)_{i+1/2}}{(r\phi\rho C_p)_i\Delta r}]T_{i+1}^n+\frac{\Delta t}{(\phi\rho C_p)_i}Q(T_i^n)$$

The weighted factor Θ is set equal to 0.75. A more computational form of equation (9a) is written as:

$$A_iT_{i-1}^{n+1}+B_iT_i^{n+1}+C_iT_{i+1}^{n+1}=D_iT_{i-1}^n+E_iT_i^n+F_iT_{i+1}^n+\left(\frac{\Delta t}{(\rho C_p)_i}\right)Q(T_i^n) \qquad (9b)$$

Convective boundary nodes

The convective boundaries at the external surface ($r = r_o$ or $r = r_s$) of the whole tree elements, using the general diffusion equations (8) are evaluated as:

$$\phi\rho C_p\left.\frac{\partial T}{\partial t}\right|_s+\lambda(T)\left.\frac{\partial T}{\partial r}\right|_s=\frac{1}{r}\frac{\partial}{\partial r}\left.(rK\frac{\partial T}{\partial r})\right|_s+Q(T)|_s \qquad (10)$$

Expanding, collecting terms and equating $K\left.\frac{\partial T}{\partial r}\right|$ respectively to the convective boundaries relations of equations (1) and (3), that is

$$K\left.\frac{\partial T}{\partial r}\right|_o=h(T_g-T(r,t))\Big|_o \quad \text{or} \quad K\left.\frac{\partial T}{\partial r}\right|_s=[\rho_w(V_s\varepsilon_s h_s+\alpha V_g\varepsilon_v h_v)+h(T_g-T_s(r,t))]\Big|_s$$

Then, discretizing the final relation as before and utilizing a fictive node inside the bed gives,

$$[1+\frac{2\Delta tK\Theta}{\phi\rho C_p\Delta r^2}T_i^{n+1}-\frac{2\Delta tK\Theta}{\phi\rho C_p\Delta r^2}T_{i-1}^{n+1}=[1-\frac{2\Delta tK}{\phi\rho C_p\Delta r^2}(1-\Theta)]T_i^n$$

$$+\frac{2\Delta tK}{\phi\rho C_p\Delta r^2}(1-\Theta)T_{i-1}^n+(\frac{\Delta t}{\phi\rho C_p})[((\frac{1}{r})_i+\frac{2}{\Delta r}-\frac{\lambda(T_i^n)}{K})\Im(T_i^n)+Q(T_i^n)] \qquad (11)$$

Where the index i identifies the boundary node and $i-1$ the internal nearest node, while $\Im(T_i^0)$ represents the respective convection boundary.

Centerline nodes

Since the same boundary conditions are applied to the external surface of the whole tree elements, the diffusion equation (8) is symmetrical about r=0. The finite difference equation is not applicable at this particular location because of singularity

problem. Making use of the symmetry boundary condition, the discretization of the appropriate expression is straightforward and yields the temperature at i=0, i.e.

$$T_o \quad \left[1+\frac{4\Delta t\Theta K}{\phi\rho C_p\Delta r^2}\right]T_o^{n+1}-\frac{4\Delta t\Theta K}{\phi\rho C_p\Delta r^2}T_1^{n+1}=\left[1-\frac{4\Delta t(1-\Theta)K}{\phi\rho C_p\Delta r^2}\right]T_o^n + \frac{4\Delta t(1-\Theta)K}{\phi\rho C_p\Delta r^2}T_1^n+\frac{\Delta t}{\phi C_p}Q(T_o^n) \tag{12}$$

MOVING BOUNDARY DISCRETIZED EQUATIONS

Moving boundary nodes

The interface (i =N), although moving has a prescribed temperature T^* and therefore is a boundary for both the shell and the core, figures 2 b. Applying equation (9b) to the core and shell nodes is straightforward, an the temperature expressions for the nearest nodes at the interface are obtained (equation 13 a for the core and 13 b for the shell).

$$A_{N-1}T_{c,N-2}^{n+1}+B_{N-1}T_{c,N-1}^{n+1}=D_{N-1}T_{c,N-2}^{n}+E_{N-1}T_{c,N-1}^{n}+(F_{N-1}-C_{N-1})T^*+\frac{\Delta t}{\phi_w\rho_w C_{pw}}Q(T_{c,N-1}^n)$$

$$B_{N+1}T_{s,N+1}^{n+1}+C_{N+1}T_{s,N+2}^{n+1}=(D_{N+1}-A_{N+1})T^*+E_{N+1}T_{s,N+1}^{n}+F_{N+1}T_{s,N+2}^{n}+\frac{\Delta t}{\phi_s\rho_s C_{ps}}Q(T_{s,N+1}^n)$$

Variable time step

The time step of the moving boundary is obtained by discretizing equation (5).

$$t_n-t_{n+1}=\Delta t_n=\frac{\rho_w\varepsilon_w h_p\Delta r^2}{K_w[T^*-T_{c,N-1}^{n+1}]-K_s[T_{s,N+1}^{n+1}-T^*]} \tag{14}$$

The core recession velocity is inferred from equation (16).

$$V_c=-\left[\frac{1}{\rho_w\varepsilon_w h_p\Delta r}\right]\left[K_w(T^*-T_{c,N-1}^{n+1})-K_s(T_{s,N+1}^{n+1}-T^*)\right] \tag{15}$$

Variable space step

The whole tree migration velocity inside the bed has been modeled by Ouédraogo et al. (2000)

$$V_f=\frac{dz}{dt}=\frac{Lr}{(1-mc)(\rho_w A_b\Phi_s)}\left(\frac{r}{r_o}\right)^p \tag{16}$$

where A_b is the bed cross section; the bed grid size is then obtained as

$$\Delta z_k=\Delta t_n\left[\frac{Lr}{(1-mc)(\rho_w A_b\Phi_s)}\left(\frac{r}{r_o}\right)^p\right] \tag{17}$$

As can be seen, equation (17) shows the dependence between the time and space steps; hence the VTSS is a hybrid model.